Control of Pump Depletion in $v_p \times B$ Acceleration of Electrons

C. W. Domier, Y. Nishida,[a] and N. C. Luhmann, Jr.
Department of Electrical Engineering, University of California, Los Angeles, Los Angeles, California 90024
(Received 15 May 1989)

Strong damping (depletion) of the driver wave (electron plasma wave) after electron acceleration has been observed in the $v_p \times B$ acceleration scheme in microwave-plasma interaction experiments. This depletion can be controlled by changing the rise time of the rf pump wave. Time- and space-resolved observations of high-energy electrons reveal the possible existence of different acceleration mechanisms near the resonance absorption layer.

PACS numbers: 52.75.Di, 52.40.Nk, 52.50.Gj

Several accelerator schemes based on lasers or short-wavelength microwaves have been proposed. One of these is a cross-field accelerator[1] (CFA) (also called a $v_p \times B$ accelerator[2,3] or a surfatron[4]), in which particles are accelerated along the wave front of a driver wave propagating perpendicularly to a static magnetic field. This phenomenon was originally predicted theoretically as a heating mechanism for ions in turbulent plasmas.[5] Clear evidence of $v_p \times B$ acceleration has been observed in microwave-plasma interaction experiments.[6-9] There are, however, several problems in realizing these accelerators. One of them is how to control pump depletion, because the wave (e.g., an electron plasma wave) suffers strong pump depletion via particle acceleration making it difficult to achieve high acceleration levels. This pump depletion has not been previously observed, to the best of our knowledge, although there are several theoretical predictions regarding it.

In this Letter, we present the first observations in microwave-plasma interaction experiments which show clear evidence of pump depletion of the excited plasma wave in the $v_p \times B$ acceleration scheme, and describe a method of control.

Experiments are performed in a pulsed, filament-discharge plasma in a cylindrical chamber (60 cm diam, 88 cm length) covered with multidipole magnets.[10] A schematic diagram of the experimental setup is shown in Fig. 1. Typical plasma parameters are $n_0 \simeq 1.2 \times 10^{11}$ cm^{-3}, $T_e \simeq 3$ eV, and $T_i \simeq T_e/10$, with an argon neutral pressure of $\approx 4 \times 10^{-4}$ Torr. The plasma is irradiated from a pyramidal horn antenna with repetitively pulsed microwaves ($f \simeq 3.15$ GHz, duration ≈ 1 μsec) up to a maximum power of 50 kW (200 W/cm^2), with a continuously variable rise time from 4 to 500 nsec ($\omega\tau = 80$–1×10^4). Here, the electron plasma wave (EPW), excited at the critical layer through a linear mode-conversion process, is used for electron acceleration. A steady-state magnetic field ($B \leq 20$ G) is produced by a pair of coils of 111 cm diam, spaced 100 cm apart. The wave electric field E_p^2 is determined with a shielded, miniature coaxial Langmuir probe (0.1 mm diam, 1 mm length). The electron energy is measured by a three-grid electrostatic energy analyzer positioned 13 cm from the mouth of the horn, facing in the $(-e)\mathbf{v}_p \times \mathbf{B}$ direction. Although the analyzer is fixed axially within the chamber, the critical layer may be moved through slight changes in plasma density, thereby permitting axial scans. A Langmuir probe situated upstream of the layer observes the ion wave streamers originating at the layer, allowing the location of the layer (corresponding to $z = 0$) to be calculated.[10]

When the nonuniform plasma is irradiated with a sharp-rise-time microwave pulse, suprathermal-electron production is observed as a result of resonance absorption.[10] In this arrangement, strong pump depletion following suprathermal-electron emission has never been observed without a static magnetic field present. Instead, the so-called "soliton flash"[11,12] or wave-breaking phenomenon has been observed near the critical layer in the unmagnetized plasma, where the amplitude of the EPW grows until a time determined by the plasma frequency and the incident microwave power at which point it decreases rapidly in amplitude coincident with hot-

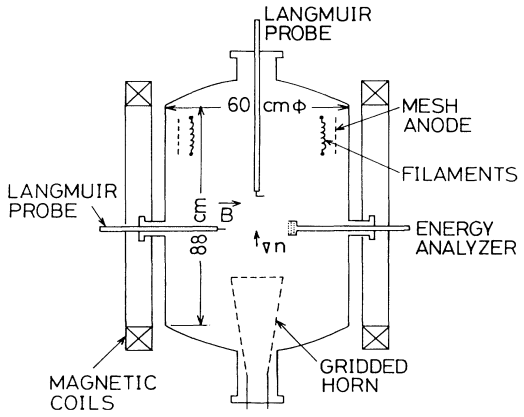

FIG. 1. Schematic diagram of the experimental apparatus. The Langmuir probe and energy analyzer located near the chamber center are oriented perpendicular to the axis of the magnet coils.

electron emission and quasi-steady-state magnetic field production.[10]

If a steady-state magnetic field is applied perpendicular to the EPW propagation direction, the $v_p \times B$ acceleration configuration is realized and strong electron acceleration is observed. An example of the maximum energy of electrons ϵ_m, accelerated as a result of this process, is shown in Fig. 2(a). An empirical best fit to the experimental results yields

$$\epsilon_m = 193 + 47.1B^2 \text{ V/cm for } B < 3.0 \text{ G}, \quad (1)$$

$$\epsilon_m = 193 + 3586/B^2 \text{ V/cm for } B > 3.0 \text{ G}. \quad (2)$$

A theoretical model for $v_p \times B$ acceleration has been developed[7] in which suprathermal electrons that become trapped in the electrostatic wave are accelerated in the $(-e)\mathbf{v}_p \times \mathbf{B}$ direction for a time $t_a \equiv (cE_p/B)/\Omega v_p$, at which point they detrap from the wave. If the wave correlation time $t_c < t_a$, however, then the electrons become detrapped earlier in time. Hence, there is a maximum energy gain $\Delta\epsilon_m \equiv \epsilon_m - \epsilon_0$ of

$$\Delta\epsilon_m = \tfrac{1}{2} m(\Omega v_p t_c)^2 = \tfrac{1}{2}(e^2/m)(v_p t_c B)^2 \text{ for } t_c < t_a, \quad (3)$$

$$\Delta\epsilon_m = \tfrac{1}{2} m(\Omega v_p t_a)^2 = \tfrac{1}{2} m(cE_p/B)^2 \text{ for } t_c > t_a, \quad (4)$$

where ϵ_0 is the maximum energy of electrons with $B=0$. Matching our empirical fit to the model, we find that $E_p \simeq 35$ V/cm, $t_c \simeq 10$ nsec, and $v_p \simeq 1.6\times10^9$ cm/sec. These results are in surprisingly good agreement with earlier results observed in a different machine at another location.[6,7]

The $v_p \times B$ electron-emission time and spatial location have been directly observed, as shown in Fig. 2(b). We have succeeded, for the first time, in obtaining time- and space-resolved observations of the high-energy electrons due to the sharp rise time of the rf pump. As clearly seen from Fig. 2(b), a high-energy electron flux I_h (with energy ≥ 100 eV) is detected $\simeq 40$ nsec after turn-on of the rf pump and is located downstream of the critical layer at $z \simeq 6$ cm. At later times of about 100 and 150 nsec, high-energy electrons are produced near the critical layer, providing evidence of different types of acceleration mechanisms as discussed in Ref. 8. Here, it should be noted that the electron-emission time is measured from the onset of the rf pulse, and is not necessarily the same as the acceleration time t_a of the $v_p \times B$ model.

Careful observations reveal that depletion of the EPW takes place when strong electron acceleration occurs, as seen in Fig. 3. Figure 3(a) shows the observed waveform of the wave, E_p^2, and the associated high-energy electron flux, I_h. These phenomena occur early in time, ≈ 40 nsec after turn-on of the rf power, and only with $B > 0$. Figure 3(b) shows a case with a longer time scale, in which pump depletion is observed early in time, while at

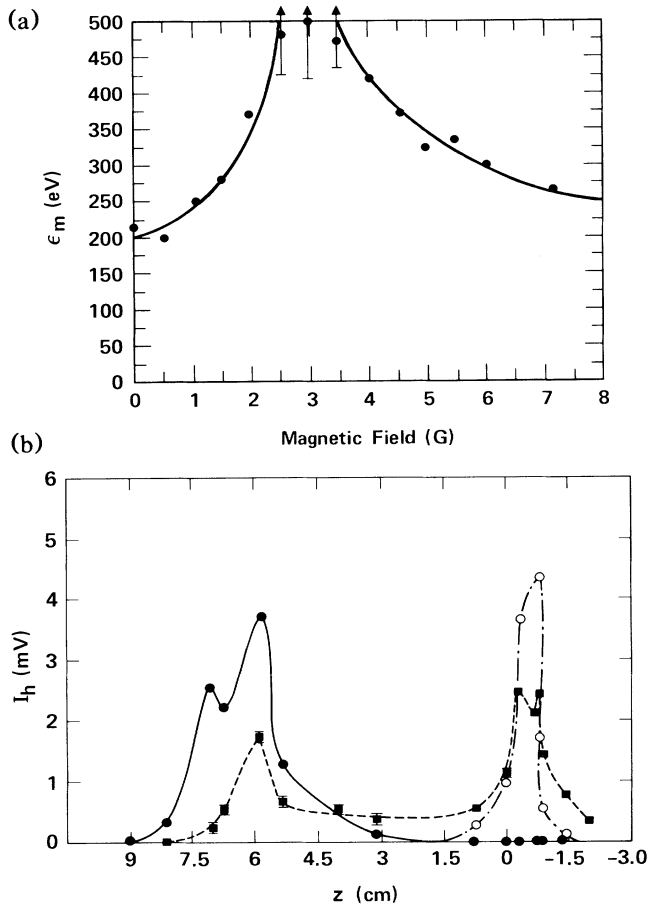

FIG. 2. (a) Maximum electron energy as a function of the magnetic field strength. $P = 2$ kW. Solid lines show the best fit to the data points. (b) Spatially resolved observations of high-energy electrons at 41 nsec (●), 101 nsec (■), 148 nsec (○) after rf pump turn-on. $P = 2$ kW and $B = 3.9$ G.

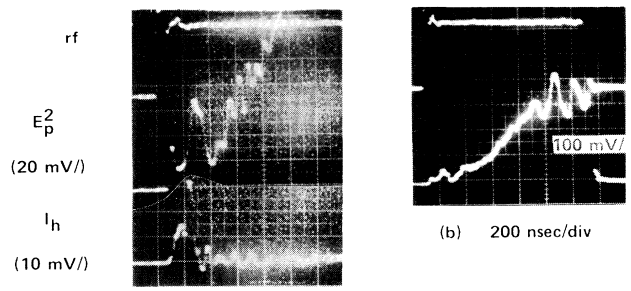

FIG. 3. (a) A typical example of EPW pump depletion and associated high-energy electron emission with an rf-pump rise time of 4 nsec. (b) An example of the time evolution of the EPW on a longer time scale. $P = 2$ kW and $B = 3.9$ G.

later times (>800 nsec) the decay instability sets in to excite ion acoustic waves.

Control of the pump depletion, occurring in the electron acceleration phase, has been investigated by varying the rise time τ_{rise} of the rf pump as illustrated by the examples shown in Fig. 4. For $\tau_{rise} \simeq 4$ nsec, strong depletion of the plasma wave occurs as shown in Fig. 4(a). The gradual increase of τ_{rise} is seen to reduce the strong depletion and a plateau regime on the plasma waveforms as seen in Figs. 4(b)–4(d). The peak value of I_h decreases as the plateau forms, and successive high-energy electron flashes take place as shown in Figs. 4(c) and 4(d). The decrement of the depletion as obtained from the results shown in Fig. 4 is displayed in Fig. 5(a), with the decrement $\Delta E^2/E_p^2$ illustrated in the inset. As clearly seen from the figure, the EPW plateau region forms when $\tau_{rise} > 60$ nsec, while the peak values of E_p^2 and I_h decrease as τ_{rise} approaches 300 nsec.

We now consider the physical mechanism responsible for the lack of observation of successive hot-electron emission after wave depletion. When the rise time is sufficiently sharp, more electrons are trapped because of rapid wave growth and a nonlinear detuning takes place.

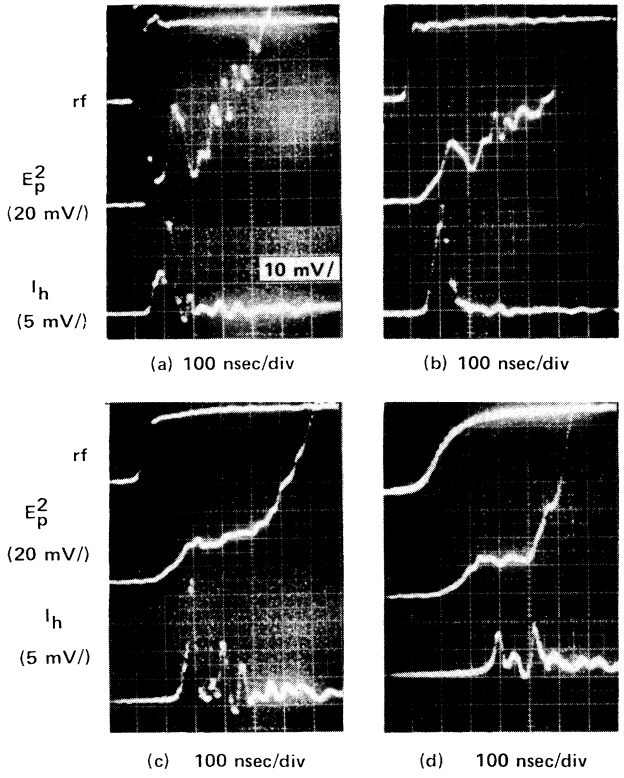

FIG. 4. A typical example of the control of EPW pump depletion and associated high-energy electron flux. The rise time of the rf pump is (a) 4 nsec, (b) 35 nsec, (c) 65 nsec, and (d) 150 nsec, respectively. $P = 2$ kW and $B = 3.9$ G.

The plasma wave then loses its coherency after a small frequency shift and pump depletion occurs such as shown in Fig. 4(a). After the depletion, the plasma wave grows turbulently because of the existence of the rf pump. On the other hand, as the slow rise time of the rf pump causes the plasma wave to be gradually saturated in amplitude (plateau regime), the coherency is retained because of weak electron loading to the wave (although there is presently no clear experimental observation) and successive bursts of accelerated electrons may occur. This is because new electrons are again trapped in the wave trough for acceleration, with sufficient wave amplitude in good coherency, after the originally trapped electrons are ejected by the initial acceleration phase. This phenomenon was suggested from results shown in Refs. 13 and 14.

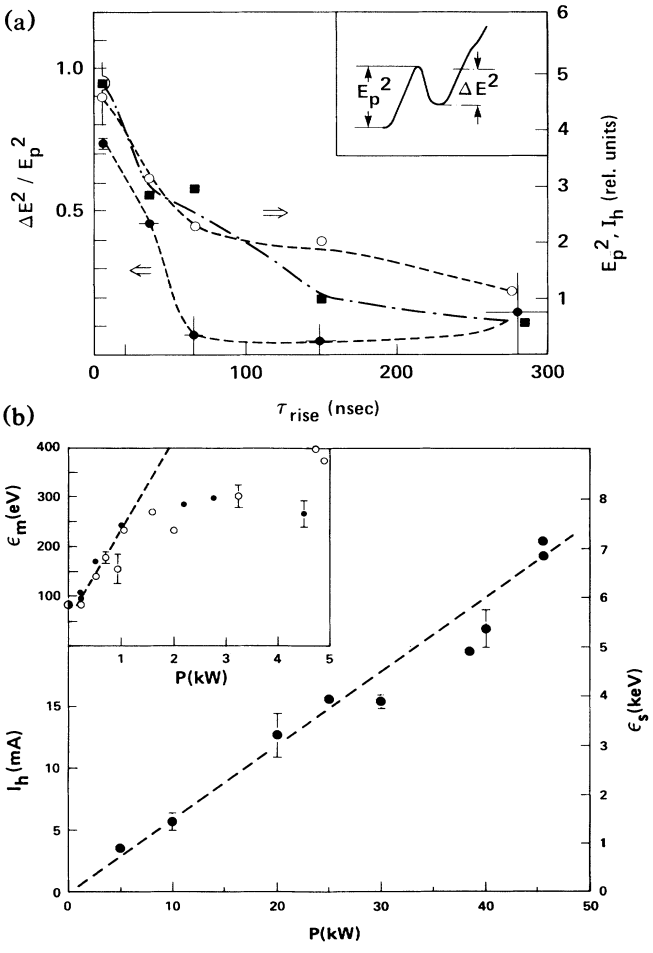

FIG. 5. (a) An example of the decrement of depletion (●), the peak electric field E_p^2 (○), and the associated hot-electron flux I_h (■) before the depletion depicted in Fig. 4. (b) High-energy electron flux I_h and estimated maximum energy ϵ_s vs microwave power. Inset: The maximum electron energy ϵ_m observed as a function of microwave power with a rise time of 4 nsec (●) and 65 nsec (○). $B = 3.9$ G.

Interestingly, the rf power dependence of ϵ_m observed at the first emission ($\simeq$40 nsec) is independent of the rise time, as shown in Fig. 5(b) where the ϵ_m of the first peak of hot-electron emission observed at a fixed position ($z \simeq 1.0$ cm, $r = 6.4$ cm) are analyzed. That ϵ_m can be determined by the wave field itself is expected from the theoretical prediction: $\Delta\epsilon_m \simeq \frac{1}{2} m(cE_p/B)^2$. It should be mentioned that the threshold power level P_c, determined from several runs in the present machine, has been observed to be $\simeq$100–150 W, which is again in good agreement with previously reported work[8] in which $P_c \simeq 150$–200 W.

In low-power measurements (< 5 kW), as shown in the inset to Fig. 5(b), we observe a leveling of ϵ_m for $P \geq 1$ kW. It is believed that this apparent saturation effect is due to the proximity of the energy analyzer to the acceleration region, intercepting the highest-energy electrons while still trapped in the wave. Measurements at a slightly more distant location ($z \simeq 1.0$ cm, $r = 8.0$ cm) show a leveling for $P \geq 2$ kW. For power levels below the "saturation" level, however, we have observed an approximately linear relationship between ϵ_m and I_h. Using this to estimate ϵ_m at the higher power levels, we have studied rf power scaling for power levels up to 50 kW, as shown in Fig. 5(b), and found a linear dependence of 150 eV/kW.

In summary, we have experimentally studied $v_p \times B$ acceleration and find that the scaling of electron acceleration with rf power (≤ 50 kW) shows a linear rate of increase of $\simeq$150 eV/kW. Pump depletion of the EPW has been observed, and controlled by changes in rf-source rise time. This feature is important for understanding the mechanism of particle loading on the wave. In realizing an electron (or ion) linear accelerator based on the $v_p \times B$ scheme, pump depletion may limit the achievement of very high energies and require a multistage system to be built. Control of pump depletion by operating in the plateau region, however, provides the possibility to simplify such a complex system. Simple wavelength scaling suggests that a CO_2-based ($\lambda = 10.6\ \mu$m) CFA system should operate in the plateau region with rise times of 7–35 psec.

This work was supported by the Laser Fusion Program of the Lawrence Livermore National Laboratory. One of the authors (Y.N.) is indebted to the Ministry of Education, Science and Culture, Japan, for their help in part by the Grant-in-Aid for Scientific Research.

[a]Permanent address: Department of Electrical Engineering, Utsunomiya University, Utsunomiya, Tochigi 321, Japan.

[1]F. F. Chen, Institute of Plasma and Fusion Research, University of California, Los Angeles, Report No. PPG-1107, 1987 (to be published).

[2]Y. Nishida and R. Sugihara, *Laser Interaction and Related Plasma Phenomena* (Plenum, New York, 1986), Vol. 7, p. 803.

[3]S. Takeuchi, K. Sakai, M. Matsumoto, and R. Sugihara, IEEE Trans. Plasma Sci. **15**, 251 (1987).

[4]T. Katsouleas and J. M. Dawson, Phys. Rev. Lett. **51**, 392 (1983).

[5]R. Sugihara and Y. Midzuno, J. Phys. Soc. Jpn. **47**, 1290 (1979).

[6]Y. Nishida, M. Yoshizumi, and R. Sugihara, Phys. Lett. **105A**, 300 (1984).

[7]Y. Nishida, M. Yoshizumi, and R. Sugihara, Phys. Fluids **28**, 1574 (1985).

[8]Y. Nishida, N. Y. Sato, and T. Nagasawa, IEEE Trans. Plasma Sci. **15**, 243 (1987).

[9]Y. Nishida, *Laser Interaction and Related Plasma Phenomena* (Plenum, New York, 1986), Vol. 7, p. 811.

[10]Ann Y. Lee, Y. Nishida, N. C. Luhmann, Jr., C. Randall, M. Rhodes, and S. P. Obenschain, Phys. Fluids **29**, 3785 (1986).

[11]K. Elsasser and H. Schamel, Plasma Phys. **19**, 1055 (1977).

[12]H. Schamel and K. Elsasser, Plasma Phys. **20**, 837 (1978).

[13]J. M. Dawson, V. K. Decyk, R. W. Huff, I. Jechart, T. Katsouleas, J. N. Leboeuf, B. Lembege, R. M. Martinez, Y. Ohsawa, and S. T. Ratliff, Phys. Rev. Lett. **50**, 1455 (1983).

[14]H. Takabe, Institute of Laser Engineering, Osaka University, Quarterly Progress Report No. ILE-QPR-86-17, 1986 (unpublished), p. 34.

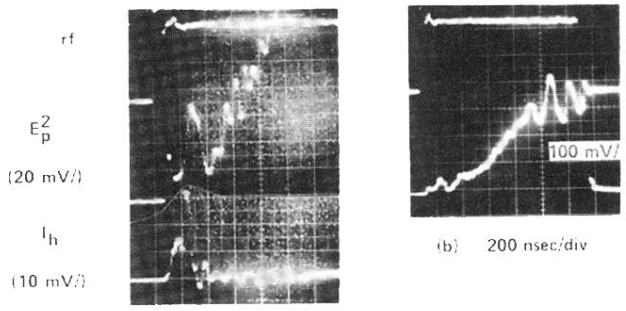

FIG. 3. (a) A typical example of EPW pump depletion and associated high-energy electron emission with an rf-pump rise time of 4 nsec. (b) An example of the time evolution of the EPW on a longer time scale. $P = 2$ kW and $B = 3.9$ G.

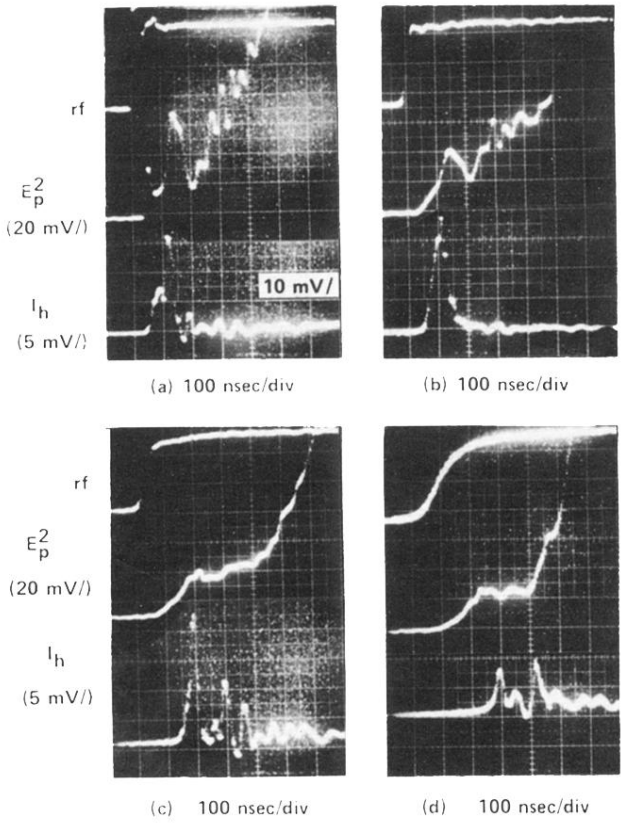

FIG. 4. A typical example of the control of EPW pump depletion and associated high-energy electron flux. The rise time of the rf pump is (a) 4 nsec, (b) 35 nsec, (c) 65 nsec, and (d) 150 nsec, respectively. $P = 2$ kW and $B = 3.9$ G.